Surface guided modes in photonic crystal ridges: the good, the bad, and the ugly

Marco Liscidini

Department of Physics, University of Pavia, Via Bassi 6, I-27100 Pavia, Italy
(e-mail: marco.liscidini@unipv.it)

Received April 24, 2012; revised June 20, 2012; accepted June 20, 2012;
posted June 22, 2012 (Doc. ID 167355); published July 23, 2012

We discuss the existence and the optical properties of guided modes in photonic crystal ridges, where light confinement relies on a photonic band gap in the direction of the substrate and on total internal reflectance in the other directions. Photonic crystal ridges are known to support guided surface waves, but here we show that at least three different guided modes can be identified, and only one of them seems to possess all the characteristics of a proper guided surface wave. We also discuss the use of effective index approaches to drastically simplify the modeling of such modes. Photonics crystal ridges are already recognized as promising platforms in the field of optical sensing and for the study of the light–matter interaction at the fundamental level, and our results should be of use in exploiting the potential of these structures for the confinement and control of light.

OCIS codes: 230.7380, 240.6690, 250.5300.

1. INTRODUCTION

The control of light propagation is central in all applications involving light–matter interaction, from classical and quantum transmission of information in optical fibers [1,2] to the use of nano devices in fundamental science [3,4]. Such a control is usually obtained by means of optical waveguides, structures in which light is forced to propagate along a given direction and confined in the other two transverse dimensions. In ordered dielectric structures, light confinement is achieved by exploiting two different effects: total internal reflection (TIR) at the interface with media having different refractive indices [5] or interference, which leads to the so-called photonic band gaps (PBGs) in photonic crystal (PhC) structures [6]. To date, several configurations supporting propagating modes confined in two dimensions have been suggested or demonstrated: optical fibers [2], ridge waveguides [7], PhC fibers [8], PhC waveguides [9], truncated PhC slabs [10], PhC wires [11], and PhC ridges [12,13]. Some of these configurations are shown in Fig. 1. On the one hand, in some structures light confinement is entirely based on a single effect, such as TIR in ridge waveguides or PBG in PhC fibers. On the other hand, the two mechanisms can be combined, for example in PhC wires, where confinement in the vertical direction is provided by a PBG, while that in the plane of the slab is given by TIR. Naturally, the confinement mechanism influences the mode characteristics, such the dispersion and field profile, and the choice of a particular structure is often driven by the specific application and the available materials. For instance, in long-distance optical communication, optical fibers have been proven to be extremely effective and robust, while the mode dispersion engineering of photonic crystal fibers is crucial to enhance nonlinear interactions in supercontinuum generation.

In this work we focus on PhC ridges [Fig. 1(b)], which are composed of a dielectric ridge placed on a one-dimensional (1D) PhC, namely a periodic multilayer. In these structures, guided modes are characterized by an asymmetric light confinement, which relies on a PBG only from the multilayer side and on TIR in all the other directions. These systems are not only appealing as platforms to develop optical sensors, but also for the study of the light–matter interaction at the fundamental level, for example in the strong-coupling regime of quantum-well excitons [13]. One of the most interesting features of PhC ridges is that one can obtain a guided mode even with ridges as thin as a few tens of nanometers. This greatly simplifies the fabrication procedure, which for some structures can be done simply by texturing the surface of multilayer structures that are commercially available.

Recently, PhC ridges have been proposed as a means to obtain guided surface waves [12,13], but here we will demonstrate the at least three different types of guide modes can be identified: we call them the *good*, the *bad*, and the *ugly*. We will show that only one of these modes, the *good*, possesses all the characteristic of a guided surface wave, while the other two, the *bad* and the *ugly*, are more similar to ridge waveguide modes, as their properties depend critically on the ridge height.

An analytic description of PhC ridges is not possible, and straightforward numerical study is not easy. Indeed, since in general the multilayered structure is characterized by numerous layers, even a hundred, whose thicknesses can be as small as a few tens of nanometers, finite-difference-time-domain (FDTD) or finite element approaches are usually time consuming, and sometimes unreliable, even in two-dimensional (2D) simulations. Moreover, even if an accurate solution can be found for a given structure, this is done at a large computation cost, and the results are not necessarily helpful towards achieving insight into the physics characterizing these modes. Here we propose a different approach, considering the fact that, in most of the cases, the ridge is sufficiently large that the vertical confinement of the electromagnetic field dominates the lateral confinement. In this limit,

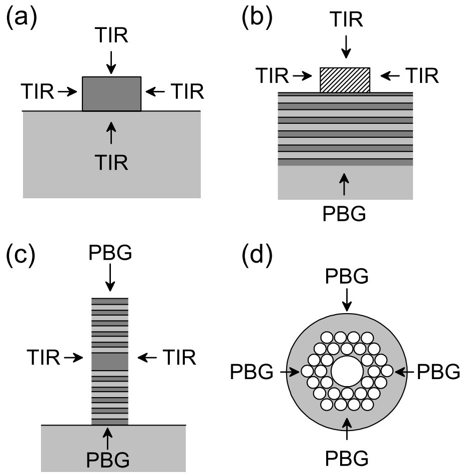

Fig. 1. Sketch of the cross sections of (a) ridge waveguide, (b) PhC ridge, (c) PhC wire, and (d) PhC fiber.

the properties of the guided modes are mainly determined by the vertical structure of the ridge, while lateral and vertical confinements can be decoupled. A similar approach is used to describe confined modes in pillar microcavities, where it has been shown that reliable results can be obtained even for pillar radius as small as 0.5 μm [14].

In Section 2 we discuss the origin and the characteristics of the typical guided modes supported by a PhC ridge, and we describe their peculiar properties. In Section 3 we show that two different effective index approaches can be used to calculate the dispersion relation of the guided modes under investigation, and we confirm by means of rigorous coupled wave analysis (RCWA) that these methods are reliable. Finally, in Section 4, we summarize our conclusions.

2. THE GOOD, THE BAD, AND THE UGLY

We consider the structure shown in Fig. 2, which is composed of a ridge of refractive index n_R, width w, and height h, on a periodic multilayer having a unit cell composed of two layers of refractive index n_a and n_b and thicknesses L_a and L_b, respectively. The multilayer truncation is defined by the first layer parameters, which are the refractive index n_a and thickness σL_a, with $\sigma \in [0, 1]$. The properties of the PhC ridge and those of its guided modes depend obviously on the multilayer

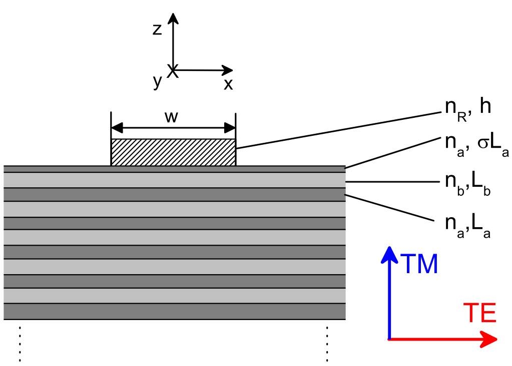

Fig. 2. (Color online) Sketch of the cross section of the PhC ridge under study.

as well as the ridge parameters. In our analysis, though, we will consider the same multilayer for all the cases under examination, letting the structure properties be determined uniquely by the choice of the ridge material and geometry. We will demonstrate that, starting from the same epitaxial structure, it is possible to obtain several types of guided modes by simply changing the ridge parameters. This will confirm the extreme flexibility of this approach to light confinement.

More specifically, we consider a multilayer made of alternating layers of $Al_{0.9}Ga_{0.1}As$ ($n_a = 2.98$) and GaAs ($n_b = 3.58$), and we work in the range between 1.1 and 1.6 eV. The first layer is 30 nm thick and made of GaAs, followed by $N = 20$ periods of a unit cell composed of a 83 nm thick $Al_{0.9}Ga_{0.1}As$ and a 69 nm thick GaAs layer. We stress out that our results do not depend on this particular material choice, and that suitable multilayers could be designed starting from different materials, having a smaller or larger refractive index contrast [15]. The structure in Fig. 2 is symmetric upon reflection with respect to the yz plane. This makes possible a classification of the modes according to their polarization or, equivalently, to the parity under mirror symmetry $\hat{\sigma}_{yz}$; the parity can be either even [$\hat{\sigma}_{yz} = +1$, transverse-magnetic (TM)] or odd [$\hat{\sigma}_{yz} = -1$, transverse-electric (TE)]. In the following calculations, we shall always consider only TE modes, for which the electric field is in the plane of the multilayer and orthogonal to the ridge.

A. The Good

The recent interest in PhC ridges comes from the study of Bloch surface waves (BSWs), which are propagation modes that can exist at the interface between a truncated PhC and a dielectric homogeneous medium [16]. In planar structures, light confinement is 1D and relies on TIR from the homogeneous material and on the PBG from the PhC side. Lately, experimental and theoretical studies that suggest the existence of guided BSWs (GBWSs) in PhC ridges has been reported [12,13]. Here it is clear that the adjective "guided" refers to the lateral confinement of the electromagnetic field provided by the ridge, but it is less obvious whether a ridge of height h can support a truly surface wave. Indeed one expects a *good* GBSW to be characterized by a dispersion relation and a mode profile that are essentially independent of h, when this is sufficiently large.

We start by considering the structure shown in Fig. 3(a), in which a 200 nm thick silica ridge ($n_R = 1.5$) is placed on the AlGaAs/GaAs multilayer. The PhC ridge can be divided in three distinct regions: the *bare* multilayers on the sides of a central region *loaded* with the silica ridge. For our parameters, both regions, when considered separately as unbounded multilayers, support a BSW. It is worth noticing that, since $n_R < n_a$, n_b, both multilayers cannot support any mode confined solely by TIR. The BSW dispersion relations can be easily calculated by means of the transfer matrix method [5,15], and they are shown in Fig. 3(b) along with the dispersion of the multilayer PBG. Note that the PBG is identical for bare and loaded regions, as determined solely by the PhC unit cell and independent of the multilayer truncation as well as the cladding and ridge materials. Since we are dealing with modes that are confined by TIR from the air cladding and by the PBG from the multilayer side, the dispersion curves

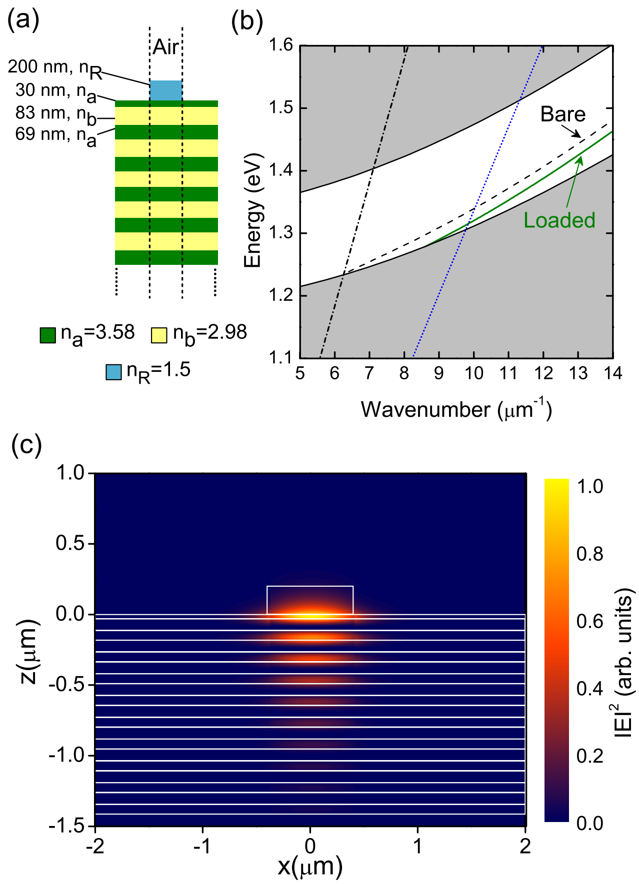

Fig. 3. (Color online) (a) Sketch of the PhC ridge of 200 nm thickness supporting a *good* mode; (b) BSW dispersion relation in the case of a bare (dash black) and loaded (solid green) multilayer. The PBG (white region) and the dispersion and light lines for air (dash dot black) and ridge material (short dot blue) are also shown. (c) *Good* mode intensity profile calculated at $\lambda = 885$ nm (1.4 eV) using the effective index approach. We consider TE-polarized light.

are below the air light line and within the PBG. The two BSWs have the same dispersion, but the mode in the loaded region is red-shifted due to the presence of the silica layer.

For w sufficiently large, one expects light to be laterally confined in the PhC ridge due to the effective index mismatch of the two modes propagating in bare and loaded multilayers. The situation is similar to what happens in shallow ridge waveguides, where 2D light confinement is obtained in thin ridges that perturb the guided modes of a slab waveguide [5]. Such a gentle confinement suggests the study of GBSW by means of an effective index approach.

We consider $\lambda = 885$ nm (1.4 eV), for which the BSWs in the empty and loaded regions have refractive indices $n_{\text{empty}} = 1.664$ and $n_{\text{load}} = 1.742$, respectively. The effective index of the guided modes can be calculated by considering an effective symmetric slab waveguide with $n_{\text{core}} = n_{\text{load}}$ and $n_{\text{clad}} = n_{\text{empty}}$ (see Section 3). In particular, for a ridge of width $w = 0.8$ μm, we find one guide mode having effective index $n_{\text{good}} = 1.711$.

Using the same approach, one can also obtain the corresponding 2D mode profile, where the 1D mode profile of the effective slab yields the correct horizontal distribution, and the 1D mode profiles of the bare and loaded BSWs give the vertical distribution in the central and lateral regions, respectively. In Fig. 3(c), we plot the intensity distribution of the modes found for $\lambda = 885$ nm. A similar result has been reported in [13], where strong coupling between a GBSW and quantum-well exciton is theoretically predicted using RCWA. In particular, since our structure is essentially that of [13], the two intensity profiles are almost identical. In both cases, we are in the presence of modes having all the characteristics of a GBSW: (1) they are confined in two dimensions; (2) the fields are peaked at the interface between the periodic structure and the ridge; (3) any vertical cross section of the mode profile in the ridge corresponds to that of a 1D BSW.

It is interesting to consider the case of an infinitely thick ridge [see Fig. 4(a)], where the analysis of the structure can be done as in the previous case. In Fig. 4(b), we show the dispersion relation of the BSWs supported by the bare and loaded multilayers. The former is obviously identical to that of Fig. 3(b), and the latter now has the cutoff below the silica light line, since the cladding material is indeed silica. Note that also the loaded mode does not differ too much from that shown in Fig. 3(b). In particular, the effective index at $\lambda = 885$ nm is essentially identical to the previous case. In Fig. 4(c), we show the corresponding mode profile, which is barely distinguishable from the one presented in Fig. 3(c), although here the ridge is semi-infinite. This confirms that

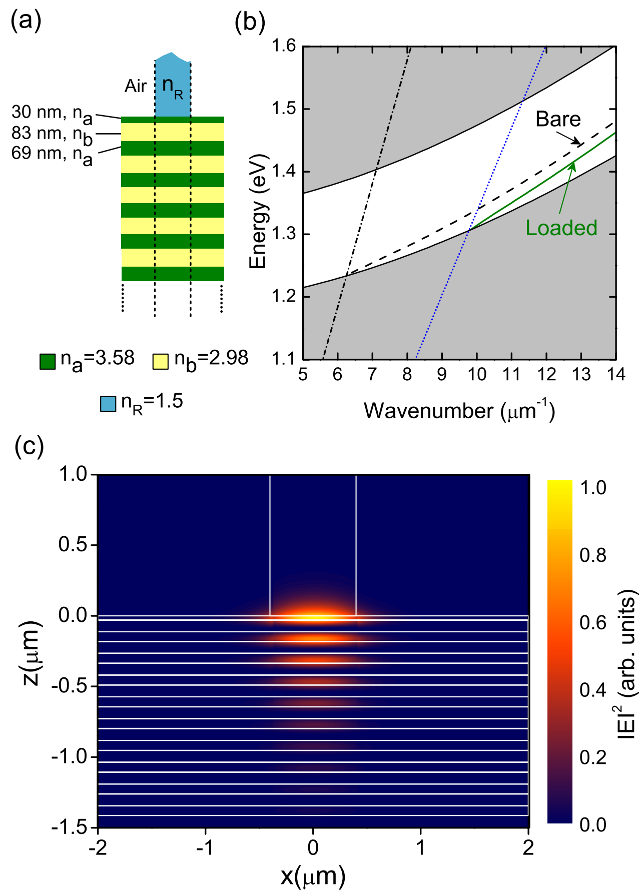

Fig. 4. (Color online) (a) Sketch of the infinitely thick PhC ridge supporting a *good* mode; (b) BSW dispersion relation in the case of a bare (dash black) and loaded (solid green) multilayer. The PBG (white region) and the light lines for air (dash dot black) and ridge material (short dot blue) are also shown. (c) *Good* mode intensity profile calculated at $\lambda = 885$ nm (1.4 eV) using the effective index approach. We consider TE-polarized light.

we are in the presence of a truly guide surface wave, whose properties are indeed independent of the ridge height.

B. The Bad

A pretty complete portrayal of a propagation mode, whether confined in one or two dimensions, is usually given by its dispersion relation and its field profile. The first contains all the spectral information (such as phase velocity, group velocity, group velocity dispersion, etc.), and the second describes how light is spatially distributed. Notwithstanding, two guided modes can exhibit similar dispersion relations and mode profiles, and yet be very different in nature, depending on how light confinement is obtained. The following example will illustrate this.

Let us consider the PhC ridge in Fig. 5(a), in which a silicon nitride ridge ($n_R = 2$) of width $w = 0.8\ \mu$m and $h = 30$ nm is placed on the AlGaAs/GaAs multilayer. In analogy with the previous cases, we can divide the PhC ridge in three slices, with and without the ridge, and calculate the dispersion curves of the guided modes supported by the two multilayers. Again, since $n_R < n_a, n_b$, any guided mode must be searched for within the PBG, as light cannot be confined solely by TIR. The results are shown in Fig. 5(b). Here, the only difference with respect to Fig. 3(b) is the dispersion of the mode in the *loaded* case. Interestingly, for most of the spectrum, the mode dispersion relation given by the 30 nm silicon nitride layer is almost identical to that obtained for a 200 nm (or infinite) silica ridge. Nevertheless, regardless of this strong resemblance, the natures of these two modes are rather different. In the structure with the silica ridge, the guided mode lies almost completely below the silica light line, and thus the field is evanescent in the silica layer. On the contrary, the dispersion relation in Fig. 5(b) is above the silicon nitride light line, and thus the field is propagating in the silicon nitride layer. The difference between the two cases is clear if we consider that there would be no guided mode in the silicon nitride structure were the height of the layer infinite, while there would be in the silica structure.

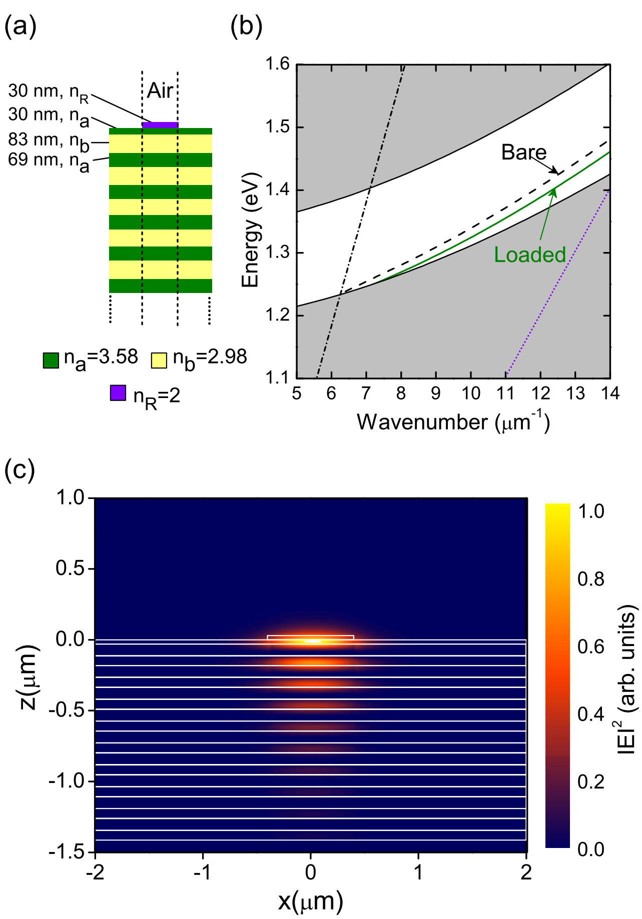

Fig. 5. (Color online) (a) Sketch of the PhC ridge supporting a *bad* mode; (b) BSW dispersion relation in the case of a bare (dash black) and loaded (solid green) multilayer. The PBG (white region) and the light lines for air (dash dot black) and ridge material (short dot purple) are also shown. (c) *Bad* mode intensity profile calculated at $\lambda = 885$ nm (1.4 eV) using the effective index approach. We consider TE-polarized light.

One expects to find a guided mode also in the PhC ridge of Fig. 5(a). Following the same effective index approach adopted above, we consider $\lambda = 885$ nm (1.4 eV) at which the BSWs in the empty and loaded regions have a refractive indices $n_{\text{empty}} = 1.664$ and $n_{\text{load}} = 1.737$, respectively. If we consider a ridge of width $w = 0.8\ \mu$m, we find a guided mode with effective index $n_{\text{bad}} = 1.708$, whose mode profile is shown in Fig. 5(c). Not surprisingly, the result is very similar to the one shown in Fig. 3(c) for the *good* mode. In particular, if the structure profiles were removed from the two figures, one could barely distinguish the two cases, which might be easily confused. In this case, we could say that the field profile shown in Fig. 5(c) is that of a *bad* surface guided mode. As a matter of fact, the field is not evanescent in the silicon nitride ridge, and light is confined nearby the multilayer surface only because the ridge thickness is small. Unlike the *good* case, this guided mode would not exist in a infinitely thick ridge.

The case we have just described is analogous to that presented by Descrovi *et al.* [12], where we would argue the term GBSW has been misused, as it does not describe the true nature of the guided mode under investigation. Nevertheless, as we emphasize by the use of the adjective “bad,” the situation is a bit subtle in that it is easy to confuse such a structure with a true GBSW. And notwithstanding this somewhat derogatory adjective, the structure demonstrated by Descrovi *et al.* finds important applications, for example in optical sensing, due to the high sensitivity of the dispersion relation of this mode to any modification of the ridge surface.

C. The Ugly

We consider now the case of a silica ridge of width $w = 0.8\ \mu$m and height $h = 0.5\ \mu$m [see Fig. 6(a)]. In Fig. 6(b), we plot the dispersion relations of the guided modes supported by the bare and loaded multilayers considered as unbounded structures. For the bare multilayer the situation is obviously identical to those presented in the previous examples: the structure supports only a BSW mode. On the contrary, in the case of the loaded multilayer, there exists a BSW [identical to that shown in Figs. 4(b) and 5(b)] and a guided mode, whose dispersion is in the region between the air and silica light lines. Note that, while the *good* and *bad* modes of the loaded structure are a perturbation of the BSW of the empty multilayer, here we are in the presence of a new mode whose existence depends on the silica layer thickness. Indeed, such a solution was not found for a 200 nm thick silica layer, nor for an infinitely thick silica layer.

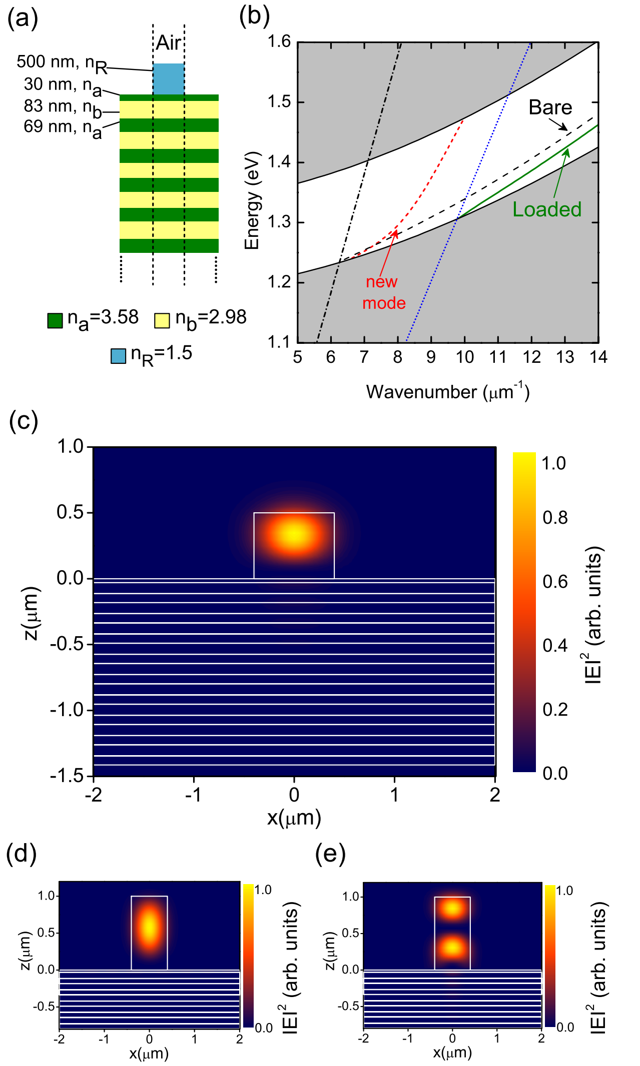

Fig. 6. (Color online) (a) Sketch of the PhC ridge with a silica ridge of height $h = 500$ nm; (b) core mode dispersion (dot red) and BSWs dispersion relations in the case of a bare (dash black) and loaded (solid green) multilayer. The PBG (white region) and the light lines for air (dash dot black) and ridge material (short dot blue) are also shown. (c) First-order *ugly* mode intensity profile at $\lambda = 885$ nm (1.4 eV) for $h = 500$ nm; (d) first-order *ugly* mode intensity profile for $h = 1$ μm; (e) second-order *ugly* mode intensity profile for $h = 1$ μm. All the modes profiles were calculated using RCWA. We consider TE-polarized light.

This analysis suggests that a guided mode, originated by that existing between the silica and air light lines, might exist in the PhC ridge.

In this case the effective index approach adopted in the previous cases cannot be applied, but we can model the structure by means of RCWA [17,18], which allows an exact description of the PhC ridge by considering the structure with periodic boundary conditions [19]. Here we took a unit cell having period of $\Lambda = 10$ μm.

In Fig. 6(c), we show the calculated intensity profile of the PhC ridge guide mode corresponding to the new structure, where we took $\lambda = 885$ nm. The calculated effective index is $n_{\text{ugly}} = 1.22$, which is close to that of the *new* mode supported by the unbounded loaded multilayer ($n_{\text{new}} = 1.30$) [see Fig. 6(b)]. The mode profile shown in Fig. 6(c) is completely different than those shown in Figs. 4(c) and 5(c). The field distribution resemblances that of a typical ridge waveguide, and the light is almost totally confined within the silica ridge. We stress that, although field oscillations are not visible in the multilayer portion of figure, light confinement from the multilayer side is still provided by the PBG as $n_{\text{ugly}} < n_a, n_b$.

We refer to this mode as *ugly*, since it is immediately clear from its intensity profile that here we are not dealing with a GBSW but with a different mode type. Unlike the *good* and the *bad* cases, the existence of *ugly* guided modes depends on the ridge height. On the one hand, the examples discussed above indicate that there exists a critical ridge height below which there is not any *ugly* mode. On the other hand, one expects that when the ridge thickness is further increased above this critical height, other modes appear. In Figs. 6(d) and 6(e), we plot the intensity profile of the first- and second-order modes for $h = 1$ μm. These results confirm that the behavior of *ugly* modes is similar to that of guide modes in wire waveguides, with the only difference that in PhC ridges the confinement from the multilayer side is provided by the PBG.

3. EFFECTIVE INDEX APPROACH IN PHC RIDGES

All the examples provided above show that PhC ridges are an extremely flexible approach to light confinement. Indeed, several types of guided modes can be found, and their dispersion can be tailored by changing the ridge as well as the multilayer parameters. Yet, the price of this versatility is the complexity of the structure, the optical properties of which depend on a number of parameters. In this respect, numerical approaches such as FDTD or RCWA are useful in the description of a specific structure, but they are often too time consuming to design and optimize a PhC ridge. To this end, one might want to rely on approaches that are faster and easier to implement. As we have seen in the previous examples, one possibility is the use of effective index approaches, which allows for the reduction of the dimensionality of the problem. In this section we show that *good*, *bad*, and *ugly* modes can be indeed efficiently described using effective index approaches.

Let us consider first the case of the *bad* mode, in which the confinement arises from a perturbation of the BSW supported by the bare multilayer. In this case, the calculation of mode profile and dispersion relation can be done using two different effective index approaches. In the former, one considers the ridge structure as a symmetric 1D effective slab [see Fig. 7(a)], where the effective index of core n_{core} and cladding n_{clad} are those of the modes supported by the bare and loaded multilayer, respectively. This idea is the one used above, and it is the same strategy usually adopted to describe shallow ridge waveguides [5].

In a second approach, one starts by looking for the guided mode supported by the symmetric slab waveguide of width w corresponding to the horizontal cross section of the layer containing the ridge. Then one substitutes the ridge region of height h with a uniform layer having the effective index corresponding the slab waveguide mode and looks for the modes supported by the effective multilayer structure [see Fig. 7(b)]. Note that in this case, depending on the ridge width and its refractive index, one in general might find several guided modes for the effective slab waveguide. In this case, each

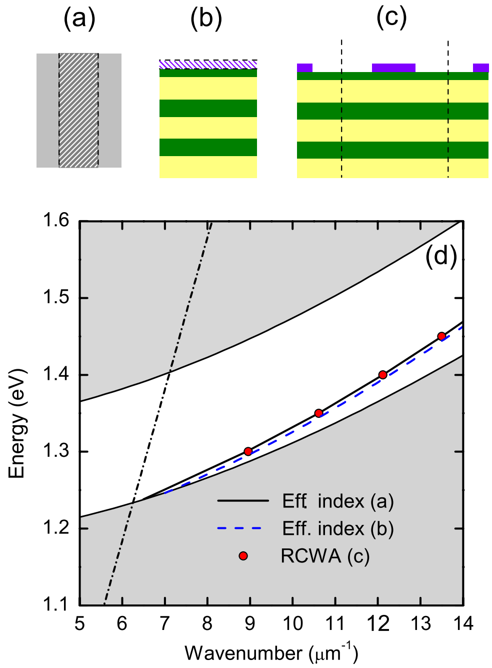

Fig. 7. (Color online) Illustration of the calculations methods: (a) vertical effective index approach, (b) in-plane effective index approach, and (c) RCWA. (d) Calculated dispersion curve of the *bad* guide mode: vertical effective index approach (solid black), in-plane effective index approach (dash blue), and RCWA (points). The PBG (white region) and the light lines for air (dash dot black) are also shown. We consider TE-polarized light.

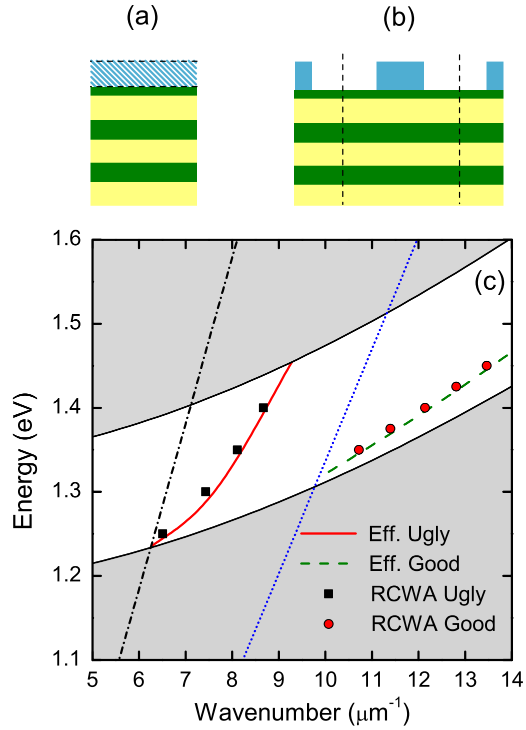

Fig. 8. (Color online) Illustration of the calculations methods: (a) in-plane effective index approach and (b) Rigorous-coupled-wave-analysis; (c) Calculated dispersion curve of the *Ugly* guided mode (in-plane effective index approach (solid black) and RCWA (squares)) and the *Good* guided mode (in-plane effective index approach (dash greed) and RCWA (circles)); The PBG (white region) and the ridge material (short dot blue) are also shown. We consider TE-polarized light.

of them will give rise to one or more modes in the multilayer structure, depending on the ridge thickness. This method has been proved particularly effective to describe high-contrast photonic wires, and it can be applied in a more general situation than the first procedure, as it does not require a perturbative approach [19].

The dispersion relations calculated using the two effective index methods are plotted in Fig. 7(d) along with those evaluated using the RCWA, in which the structure is calculated assuming a periodic boundary condition [see Fig. 7(c)]. There is a good agreement between the RCWA results and the dispersion curves obtained using the first effective index method. This is not surprising, given the perturbative nature of the mode under investigation. On the contrary, the second effective index approach gives a slightly shifted dispersion relation. As a matter of fact, this approach is particularly effective when the electromagnetic field is strongly confined in the ridge region [19]. Notwithstanding the fact that this is not the case [see Fig. 5(c)], we can still say that the agreement with the other results is rather good.

To complete our analysis, we consider also the case of a 500 nm silica ridge of Fig. 6(a), which supports both the *good* and the *ugly* modes. In this case, the effective index method illustrated in Fig. 7(a) cannot be applied to calculate the dispersion of the *ugly* mode, as it does not originate from a perturbation of the BSW of the bare multilayer. Yet, we can still use the second effective index approach [Fig. 7(b)], which seems to be particularly indicated to describe this kind of mode given the strong light confinement in the ridge [see Figs. 6(c), 6(d), and 6(e)]. The dispersion curves of both the *ugly* and *good* modes (lines) are shown in Fig. 8(c), together with the RCWA results (points). The good agreement between the curves and the points indicate that also these modes can be effectively described within the effective index theory. For each mode, we found a good agreement also for the field intensity distributions at specific energies (not shown).

As usual when one deals with effective index methods, the accuracy and effectiveness of the approach depend upon the geometrical parameters of the structure, the material refractive indices, and the frequency range under investigation. In this respect, this analysis cannot be considered exhaustive, but it gives a flavor of the possible routes that can be followed in the study of PhC ridges. We stress that, unlike Fourier modal methods or other numerical techniques, e.g., FDTD, these effective index approaches take only minutes, if not seconds, on a standard personal computer. This allows for a quick inspection of the vast parameter space and a drastic reduction of the time required for the design and optimization of a PhC ridge for a specific application.

4. CONCLUSIONS

We discussed the existence of surface guided modes in PhC ridges. Starting from the same multilayer structure, we have been able to theoretically demonstrate the existence of three different types of guided modes. First, the *good*, which is indeed a GBSW, propagating at the interface between a truncated periodic multilayer and a dielectric ridge. We showed that, for a sufficiently thick ridge, the properties of this mode are independent of the ridge thickness, even when this is assumed to be infinite. Second, the *bad*, which is not a surface mode, despite the fact that its dispersion relation and field distribution can be similar to those of a GBSW; like the *good*, it originates from a perturbation of a BSW, but its properties depend on the ridge thickness. And finally, the *ugly*, which is reminiscent of a guided mode in photonic wires, although light confinement is based on both TIR and a PBG. Unlike *bad* modes, it exists only for a sufficiently large ridge thickness.

We showed that *good*, *bad*, and *ugly* modes can be described by means of effective index theories. We compared our approximate results with those obtained by means of RCWA, demonstrating that these effective index methods can be used to calculate both the mode dispersion and the field profile. With the fast and easy implementation of such effective methods, the design and optimization of PhC ridge waveguides can be greatly simplified.

We believe such results might stimulate new interest in PhC ridges, which are certainly an appealing and flexible platform to develop integrated devices for several applications, ranging from fundamental research to applied science.

ACKNOWLEDGMENTS

This work is supported by the Italian Ministry of University and Research, Fondo per gli investimenti della ricerca di base (FIRB) Contract No. RBFR08QIP5, and the foundation Alma Mater Ticinensis. The author is grateful to Lucio Andreani, Daniele Bajoni, Stefano Pirotta, and J. E. Sipe for stimulating discussions and the critical reading of the manuscript. Thanks to John Sipe for the suggestion of such an effective title.

REFERENCES

1. I. Marcikic, H. de Riedmatten, W. Tittel, H. Zbinden, and N. Gisin, "Long-distance teleportation of qubits at telecommunication wavelengths," Nature **421**, 509–513 (2003).
2. F. P. Kapron, D. B. Keck, and R. D. Maurer, "Radiation losses in glass optical waveguides," Appl. Phys. Lett. **17**, 423–425 (1970).
3. C. Xiong, C. Monat, A. S. Clark, C. Grillet, G. D. Marshall, M. J. Steel, J. Li, L. OFaolain, T. F. Krauss, J. G. Rarity, and B. J. Eggleton, "Slow-light enhanced correlated photon pair generation in a silicon photonic crystal waveguide," Opt. Lett. **36**, 3413–3415 (2011).
4. E. Wertz, L. Ferrier, D. D. Solnyshkov, R. Johne, D. Sanvitto, A. Lematre, I. Sagnes, R. Grousson, A. V. Kavokin, P. Senellart, G. Malpuech, and J. Bloch, "Spontaneous formation and optical manipulation of extended polariton condensates," Nat. Phys. **6**, 860–864 (2010).
5. A. Yariv and P. Yeh, *Photonics* (Oxford University, 2007).
6. J. D. Joannopoulos, S. G. Johnson, J. N. Winn, and R. D. Meade, *Photonic Crystals Molding the Flow of Light*, (Princeton University, 1st ed.: 1995, 2nd ed.: 2008).
7. I. P. Kaminow, V. Ramaswamy, R. V. Schmidt, and E. H. Turner, "Lithium niobate ridge waveguide modulator," Appl. Phys. Lett. **24**, 622–625 (1974).
8. P. Russell, "Photonic crystal fibers," Science **299**, 358–362 (2003).
9. S. J. McNab, N. Moll, and Yu. A. Vlasov, "Ultra-low loss photonic integrated circuit with membrane-type photonic crystal waveguides," Opt. Express **11**, 2927–2939 (2003).
10. Y. A. Valsov, N. Moll, and S. J. McNab, "Observation of surface states in a truncated photonic crystal slab," Opt. Lett. **29**, 2175–2177 (2004).
11. P. Yeh and A. Yariv, "Bragg reflection waveguides," Opt. Commun. **19**, 427–430 (1976).
12. E. Descrovi, T. Sfez, M. Quaglio, D. Brunazzo, L. Dominici, F. Michelotti, H. P. Herzig, O. J. F. Martin, and F. Giorgis, "Guided Bloch surface waves on ultra-thin polymeric ridges," Nano Lett. **10**, 2087–2091 (2010).
13. M. Liscidini, D. Gerace, D. Sanvitto, and D. Bajoni, "Guided Bloch surface wave polaritons," Appl. Phys. Lett. **98**, 121118–121120 (2011).
14. J. M. Gerard, D. Barrier, J. Y. Marzin, R. Kuszelewicz, L. Manin, E. Costard, V. Thierry Mieg, and T. Rivera, "Quantum boxes as active probes for photonic microstructures: the pillar microcavity case," Appl. Phys. Lett. **69**, 449–451 (1996).
15. M. Liscidini and J. E. Sipe, "Analysis of Bloch-surface-wave assisted diffraction-based biosensors," J. Opt. Soc. Am. B **26**, 279–289 (2009).
16. P. Yeh, A. Yariv, and A. Y. Cho, "Optical surface waves in periodic layered media," Appl. Phys. Lett. **32**, 104–106 (1978).
17. D. M. Whittaker and I. S. Culshaw, "Scattering-matrix treatment of patterned multilayer photonic structures," Phys. Rev. B **60**, 2610–2618 (1999).
18. M. Liscidini, D. Gerace, L. C. Andreani, and J. E. Sipe, "Scattering-matrix analysis of periodically patterned multilayers with asymmetric unit cells and birefringent media," Phys. Rev. B **77**, 035324 (2008).
19. P. Bienstman, S. Selleri, L. Rosa, H. P. Uranus, W. C. L. Hopman, R. Costa, A. Melloni, L. C. Andreani, J. P. Hugonin, P. Lalanne, D. Pinto, S. S. A. Obayya, M. Dems, and K. Panajotov, "Modelling leaky photonic wires: A mode solver comparison," Opt. Quantum Electron. **38**, 731–759 (2006).